26^{th} EPS Conf. on Contr. Fusion and Plasma Physics, Maastricht, 14 - 18 June 1999 ECA Vol.23J (1999) 1577 - 1580

Reconstruction of two-dimensional emissivity distributions in the ASDEX Upgrade LYRA-Divertor from TV-CCD-Data

J. Gafert, K. Büchl, M. E. Fenstermacher†, W. H. Meyer† and ASDEX Upgrade Team

MPI für Plasmaphysik, EURATOM Association, D-85748 Garching, Germany

†*Lawrence Livermore National Laboratory, P.O.Box 808, Livermore, CA–94550, USA*

1 Introduction

Enhanced radiation in the divertor region has proven to be an efficient way to reduce the heat load onto the divertor target plates to values tolerable from an engineering point of view [1]. A prerequisite for further expanding the knowledge on the related physics of detachment, recombination and recycling is a profound experimental characterization of both the composition and the spatial distribution of the emission.

At ASDEX Upgrade this was done until now by mainly making use of the 2D-radiation profiles from bolometry in combination with the data from a versatile fiberoptic multichord spectroscopy system [2]. In order to get 2D-distributions for relevant emission lines (CIII, H_α, etc.) routinely and in the whole divertor region including the X-point, a technique is being implemented for ASDEX Upgrade Divertor II (LYRA) that has been first introduced at DIII-D [3]. By using the chord integrated pixel-data of a CCD-camera viewing the divertor tangentially and a geometry matrix containing the information about the field of view and the renderings of the divertor the 2D-emission distribution in a poloidal plane is reconstructed by a linear least squares fitting routine.

In this paper we will shortly review some principles of this reconstruction technique and then describe its application to ASDEX Upgrade and the specific features arising due to the deep and narrow geometry of the LYRA divertor. Then the first results for reconstructed CIII-profiles (for a well characterized discharge) will be presented and discussed. The last section deals with further improvements to be implied to make the technique work reliably and routinely.

2 Experimental Setup and Principles of Matrix Inversion

The principle of ASDEX Upgrade's video diagnostics system is sketched in Fig. 1. The visible plasma radiation is collected and imaged onto a CCD-chip (582 $\times$ 752 pixels) using an image guide and appropriate lenses and filters. The images are transferred to and recorded by a video tape recorder at a rate of 25 frames per second. As a preparation for the data evaluation, the CCD-data are currently digitized to TIFF-format from video tape with a frame grabbing system.

The X-point camera view into the LYRA divertor, as calculated from CAD-data of ASDEX Upgrade, is shown in the left part of Fig. 2. Despite the deep slots all the possible emission regions are in the field of view, though they are not weighted homogeneously in the image of the CCD-camera.

The reconstruction technique presented here is based on the calculation of a response-function-matrix (= "geometry matrix", M) that contains the geometric information about the field of view of each CCD-pixel and about the material structures limiting the corresponding lines of sight. Assuming toroidal symmetry, the 2D-emissivity distribution ($\vec{A}$) is

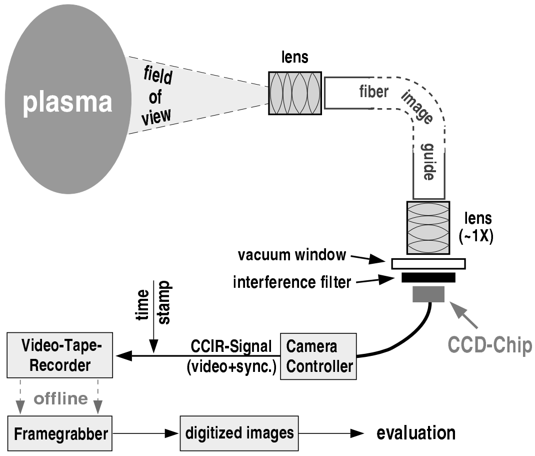

Figure 1: *Scheme of the video diagnostic data acquisition system at ASDEX Upgrade. Currently, 12 CCD-cameras are recorded simultaneously. This paper focusses mainly on the X-point-camera*

then calculated from the experimental data ($\vec{B}$) in an iterative scheme only using matrix multiplications: $M \cdot \vec{A} = \vec{B}$

Taking into account the large number of pixels of a CCD-camera, this reconstruction process is much easier than other tomographic methods that work with a truely inverted matrix, which would have to be calculated iteratively here due to its large size.

The right picture in Fig. 2 has been created from the data of the geometry matrix (M), i.e. with the same data being used to reconstruct the 2D-distributions from the CCD-camera data. This picture is also employed to align the digitized images of the emission to the geometry matrix with regard to size, rotation and shift, before the reconstruction is started. This alignment, which is necessary because of the focussing optics and therefore only after a change of optics, is done according to geometric and physical arguments: Emission can e.g. only be seen in front of and not behind material surfaces. The alignment with regard to the position of emission structures is performed in several steps: From the 2D-data for the total radiated power, together with the 1D-profiles for CIII- and H_β-emission and other spectroscopic data, approximated 2D-distributions ($\vec{A}$) for CIII were derived for distinct phases of the discharge. With the synthetic CCD-images ($\vec{B}$), calculated via $\vec{B} = M \cdot \vec{A}$, the experimental CCD-images were aligned according to the prominent emission structures. After having reconstructed 2D-emission profiles from the camera data using a couple of reasonable alignments, the best case was selected with respect to the agreement of, first, reconstructed and experimental CCD-images, and sec-

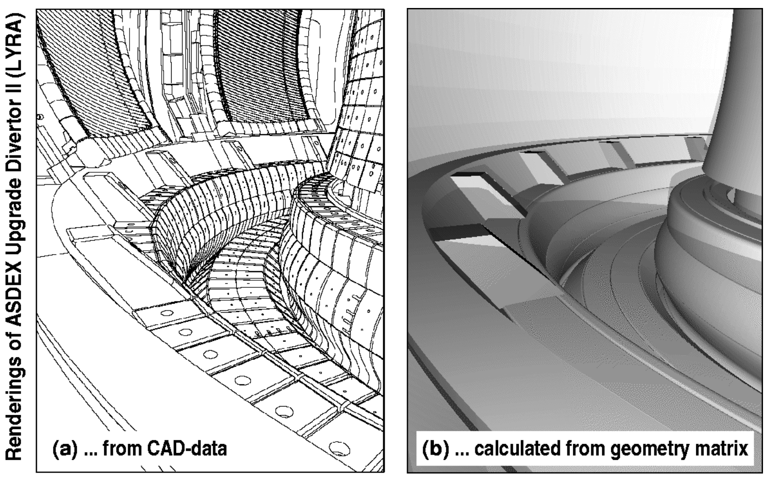

Figure 2: *The ASDEX Upgrade LYRA Divertor as seen by the tangentially viewing X-point-camera. The left image (a) was created from CAD-data, the right one (b) was calculated using the geometry matrix that has been set up on the basis of geometric information.*

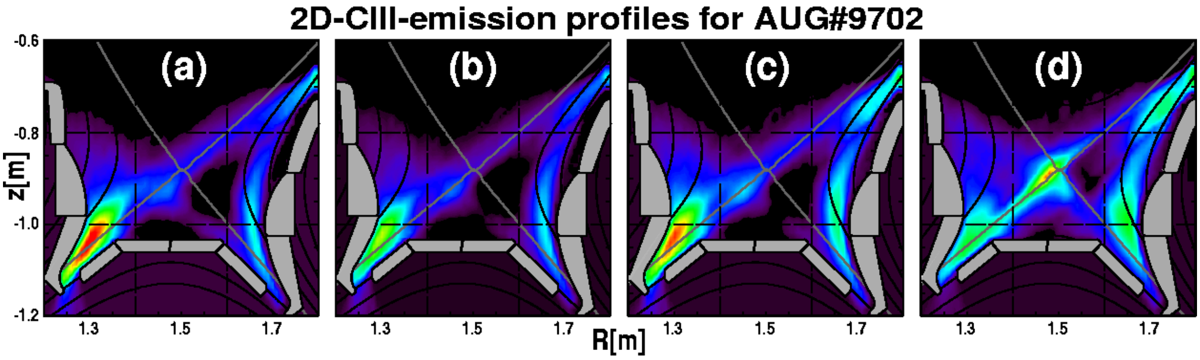

Figure 3: *Reconstruction of 2D-CIII-emission-distributions from X-point-camera data. The four times are related to different degrees of detachment and power levels. The color coding starts with black (= artificial "negative emission") and dark violet (zero emission) and ends with red (maximum emission). The same color scale is valid for each image.*

ond, of reconstructed and expected (see above) 2D-profiles.
The alignment chosen according to these and other criteria is valid for a whole period of shots with unchanged optics, because it does not depend on plasma equilibria, but only on geometry. In this context it should be mentioned that, in contrast to the case of a flat divertor (like DIII-D's), a good alignment for a deep, narrow divertor (like ASDEX Upgrade's LYRA) is much more crucial for achieving satisfactory reconstructions.

3 Test of the Reconstruction Technique: 2D-CIII-Emission-Profiles

In order to test the performance of this technique applied to the deep LYRA divertor, CCD-data for CIII-emission in L-Mode discharges with density ramps were chosen. The pronounced detachment occuring with increasing density leads to significant changes of the respective emission distributions. As for these discharges an extensive set of spectroscopic and bolometric data is available, they offer the possibility to check the quality of the reconstruction process.
Fig. 3 shows an example of reconstructed 2D-CIII-distributions (AUG#9702) for four distinct cases related to different degrees of detachment: From the experimental data it is known that Fig. 3(a) refers to a well attached plasma, whereas for (b) and (c) the plasma just begins to detach at the separatrix (from (b) to (c) the NBI-heating power was increased). For (d) the plasma is well detached as documented e.g. by an upward movement of CIII-emission measured by 1-dimensional divertor spectroscopy in front of the target plates. The 2D-reconstructions for the attached cases (a, b, c) show — as expected both from B2-EIRENE-modelling and from spectroscopic data — that the CIII-emission maxima are localized in the divertor slots near the strike points with only little intensity in the vicinity of the X-point. The increase of CIII-intensity from (b) to (c) is due to the increase of the heating power. In going to the well detached case (d) two changes are obvious: While CIII-intensity has decreased clearly in the lower regions near the strike-point plates, it is significantly enhanced near the X-point and in regions situated more upstream in the outer divertor. This is also in agreement with the total radiated power from bolometry and with the 1D-spectroscopic data. We would like to note here that these 2D-CIII-profiles further support the interpretation of flow reversal in the ASDEX Upgrade Divertor II we presented recently [4]: The reversed flow of C^{2+}-ions can only

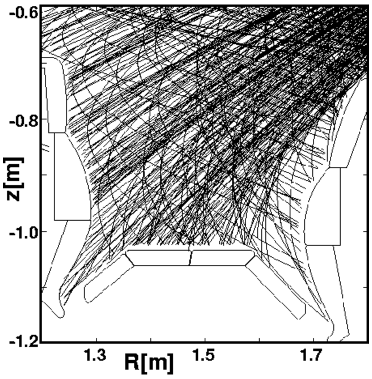

Figure 4: *Projections of the lines of sight of the tangentially viewing X-point-CCD-camera into a poloidal plane. For clarity of the picture only a reduced amount of chords (1.268), selected randomly out of the total number of 50.700, is plotted. In the deep divertor slots there are not enough chords crossing each other sufficiently to enable a resolution in z-direction.*

be detected, if there is enough CIII-emission in the flow reversal regions located more upstream, i. e. if the degree of detachment is sufficiently high.
However, beside this good reproduction of the overall emission structures, there is one main feature that is not satisfactory yet: The peaking of CIII-emission near the strike points in the attached cases — as known from the 1D-CIII-profiles — can not be reconstructed from the tangentially viewing X-point camera alone. The reason for this stems from the narrowness of the LYRA-divertor (comp. Fig. 2) and is evident from the projections of a subset of CCD-chords into a poloidal plane (Fig. 4): First, the amount of CCD-chords viewing these deep-lying regions is — especially in the outer divertor — rather low, and second, there are — due to the tangential view — not enough chords crossing each other effectively enough to yield a resolution in z-direction. Hence, intensity variations along the target plates can not be recovered by using these data only.
If the outer strike-point is, however, located on the horizontal part of the roof baffle, the situation is quite different: As expected from the larger number of crossed chords there (comp. Fig. 4), the reconstructed 2D-H_α-profiles for these cases show a pronounced maximum near the surface ($R \approx 1.55$ m, $z \approx -1.02$ m).

4 Improvements to be Done

In order to expand the spatial resolution to the deep regions of the divertor, two CCD-cameras viewing the inner and outer divertor poloidally will be included into the geometry matrix in a next step. These additional views supply the effective crossing of chords needed for a satisfactory tomographic reconstruction of emission.
Furthermore, the data of the CCD-cameras viewing the X-point will no longer be stored on video tape, but directly on hard disk. This leads, on the one hand, to an improvement in pixel resolution, and is, on the other hand, a prerequisite for getting reconstructions of 2D-emission profiles for each discharge routinely. With these results, the systematic investigation of the divertor radiation as well as the comparison to B2-EIRENE modelling will be strongly improved.

References

[1] Kallenbach, A. et. al., Nuclear Fusion, in press.
[2] Gafert, J. et. al., ECA (Proc. of the 24^{th} EPS-Conf.), **21A/IV**, 1397–1400 (1997).
[3] Fenstermacher, M.E. et. al., Rev. Sci. Instrum., **68**, 974 – 977 (1997).
[4] Gafert, J. et al., J. Nucl. Mat., **266–269**, 365 – 369 (1999).